III International Conference on Particle-based Methods – Fundamentals and Applications
PARTICLES 2013
M. Bischoff, E. Oñate, D.R.J. Owen, E. Ramm & P. Wriggers (Eds)

NUMERICAL SIMULATION OF SOIL-WATER JET INTERACTION WITH SMOOTHED PARTICLE HYDRODYNAMICS

Z. M. Guo *, †, J. R. Shao††, Y. X. Shen *, M. B. Liu††

*Laboratori de Càlcul Numèric (LaCàN)
Universitat Politècnica de Catalunya (UPC)
C. Jordi Girona 1-3, Campus Nord
08034 Barcelona, Spain
E-mail: guozhiming@live.cn (Guo), yongxing.shen@upc.edu (Shen)

†North University of China
Xueyuan Road 3
030051 Taiyuan, Shanxi, China
E-mail:guozhiming@live.cn

††Institute of Mechanics，Chinese Academy of Sciences
#15, Bei Si Huan Xi Lu, Haidian District, Beijing, China 100190
Email: liumoubin@imech.ac.cn

Key words: Smoothed Particle Hydrodynamics (SPH), Water Jet, Soil-Water Interaction, Elastic-Perfectly Plastic flow, Meshfree Method

Abstract. Smoothed particle hydrodynamics (SPH) is a meshfree, Lagrangian particle method, which has been applied to different areas in sciences and industrial applications. In this work, SPH is used to simulate the soil–water jet interaction and erosion. In the simulation, water is modelled as a viscous fluid with weak compressibility and the soil is assumed to be an elastic–perfectly plastic material. The stress states of soil in the plastic flow regime follow the Drucker-Prager failure criterion. Both the shear and tensile criterions are used for the yield of soil particles if the yield point is reached and the total stress of the particle is scaled. Instead of computing particle pressure from an equation of state, the spherical stress is computed by dividing total stress into spherical stress and deviatoric stress. The interaction of coupling interfaces is strengthened by a penalty function to avoid unphysical penetration between particles from different materials. The obtained numerical results have shown that SPH could be a valuable method for the simulation of complex soil water interaction.

1 INTRODUCTION

Smoothed particle hydrodynamics (SPH) is a "truly" meshfree, particle method originally used for continuum scale applications, and may be regarded as the oldest modern meshfree particle method. It was first invented to solve astrophysical problems in three-dimensional open space [1, 2], and later extended for many other problems. In SPH, particles are used to represent the state of a system and these particles can freely move according to internal particle interactions and external forces. As a Lagrangian particle method, SPH conserves mass exactly. In SPH, there is no explicit interface tracking for multiphase flows – the motion of the fluid is represented by the motion of the particles, and fluid surfaces or fluid-fluid interfaces move with particles representing their phase defined at the initial stage. The meshfree nature of SPH method remove the difficulties due to large deformations since SPH uses particles rather than mesh as a computational frame to approximate related governing equations. Therefore since its invention, SPH has been applied to a vast range of problems successfully, which include elastic–plastic flow [3, 4], quasi-incompressible flow [5], fracture of brittle solids [6], impact problems[7], fast landslide propagation[8][9] and fluid structure interactions[10], and etc.

In Geomechanics, Bui et al. first modeled the soil-water interaction[11]. In Bui's work, the saturated soil is modeled by mixing both soil particles and water particles together in the same soil domain and numerical results obtained in this study have shown that SPH could be a valuable method for simulation of complex problem in soil mechanics. Blanc et al.[12] presented a stabilized fractional step SPH algorithm which combines the advantages of the SPH method for large deformation problems with the Taylor Galerkin algorithm used within the finite element framework. Mabssout et al.[13] provided a comparison between two different time integration schemes, Runge-Kutta and Taylor-SPH, for SPH applied to soil dynamics problems.

In this paper, we shall describe the SPH modeling of soil-water interaction. Water is modelled as a viscous fluid with weak compressibility and the soil is assumed to be an elastic–perfectly plastic material. To obtain better accuracy, the SPH particle approximation algorithm has been improved with kernel gradient correction. The effectiveness of the SPH method in modeling water jet and soil-water interaction will be demonstrated in two numerical examples.

2 SPH METHODOLOGY

2.1 Basic concepts of SPH

In SPH, the state of a system is represented by a set of particles, which possess material properties and interact with each other within the range controlled by a weight function or named smoothing function *W*. An important advantage of SPH is that in SPH, there is no explicit interface tracking for multiphase or multimaterials, and free surface flows – the motion of the fluid is represented by the motion of the particles, and fluid surfaces or fluid-fluid and fluid-solid interfaces move with particles representing their phase defined at the initial stage. Therefore, SPH is attractive in modeling the soil-water interaction and erosion process.

In conventional SPH method, the values of a particular variable at any point can be obtained using following equations:[3]

$$< f(\boldsymbol{x}_i) >= \sum_{j=1}^{N} \frac{m_j}{\rho_j} f(\boldsymbol{x}_j) W(\boldsymbol{x}_i - \boldsymbol{x}_j, h) \tag{1}$$

$$< \nabla f(\boldsymbol{x}_i) >= \sum_{j=1}^{N} \frac{m_j}{\rho_j} f(\boldsymbol{x}_j) \nabla_i W_{ij} \tag{2}$$

where $< f(\boldsymbol{x}_i) >$ is the approximated value of particle i; $f(\boldsymbol{x}_j)$ is the value of $f(\boldsymbol{x})$ associated with particle j; $\boldsymbol{x}_i$ and $\boldsymbol{x}_j$ are the positions of corresponding particles; m and ρ denote mass and density respectively; h is the smooth length; N is the number of the particles in the support domain; W is the smoothing function representing a weighted contribution of particle j to particle i. The smoothing function should satisfy some basic requirements, such as normalization condition, compact supportness, and Delta function behavior[4, 5].

2.2 SPH equations of motion

For hydrodynamics of fluids and solids with material strength, the following governing equations of continuum mechanics apply

$$\begin{cases} \dfrac{\mathrm{D}\rho}{\mathrm{D}t} = -\rho \dfrac{\partial v^{\beta}}{\partial x^{\beta}} \\ \dfrac{\mathrm{D}v^{\alpha}}{\mathrm{D}t} = \dfrac{1}{\rho} \dfrac{\partial \sigma^{\alpha\beta}}{\partial x^{\beta}} \end{cases} \tag{3}$$

where the scalar density ρ, and internal energy e, the velocity component $\boldsymbol{v}^{\alpha}$, and the total stress tensor $\sigma^{\alpha\beta}$ are the dependent variables. The spatial coordinates $\boldsymbol{x}^{\alpha}$ and time t are the independent variables. The summation in equation (3) is taken over repeated indices, while the total time derivatives are taken in the moving Lagrangian frame. For fluid, the total stress tensor $\sigma^{\alpha\beta}$ in equation (3) is made up of two parts, one part of isotropic pressure p and the other part of shear stress $S^{\alpha\beta}$, The hydrodynamic pressure is computed from an equation of state (EOS). For solid materials, the total stress can be computed from the constitutive equations of corresponding materials. Therefore using above-mentioned SPH approximations, the following SPH equations of motion can be obtained

$$\begin{cases} \dfrac{d\rho_i}{dt} = \rho_i \sum_{j=1}^{N} \dfrac{m_j}{\rho_i}\left(v_i^{\beta} - v_j^{\beta}\right)\dfrac{\partial W_{ij}}{\partial x_i^{\beta}} \\ \dfrac{dv_i^{\alpha}}{dt} = -\sum_{j=1}^{N} m_j \left(\dfrac{\sigma_i^{\alpha\beta}}{\rho_i^2} + \dfrac{\sigma_j^{\alpha\beta}}{\rho_j^2} + \Pi_{ij} + F_{ij}^{n} R_{ij}^{\alpha\beta} \right) \dfrac{\partial W_{ij}}{\partial x_i^{\beta}} \end{cases} \tag{4}$$

where Π stand for the artificial viscosity; F_{ij}, R_{ij} stand for interaction force between two particles and the artificial stress coefficient respectively[4].

2.3 Kernel gradient correction

Water-soil interaction involves impact between fluid and solid materials, rapid deformation, and fracture on soil material. These will lead to highly disordered particle distribution. So it is necessary to use an SPH approximation scheme, which is of higher order accuracy and is insensitive to disordered particle distribution, to improve computational accuracy.

In this paper, the kernel gradient in SPH approximations is improved with a kernel gradient correction (KGC) technique[6]. In the KGC technique, a modified or corrected kernel gradient is obtained by multiplying the original kernel gradient with a local reversible matrix $L(\boldsymbol{r}_i)$, which is obtained from Taylor series expansion method. In two-dimensional spaces, the new kernel gradient of the smoothing function $\nabla_i^C W_{ij}$ can be obtained as follows:

$$\nabla_i^C W_{ij} = L(\mathbf{r}_i)\nabla_i W_{ij} \tag{5}$$

$$L(\mathbf{r}_i) = \left(\sum_j \begin{pmatrix} x_{ji}\dfrac{\partial W_{ij}}{\partial x_i} & y_{ji}\dfrac{\partial W_{ij}}{\partial x_i} \\ x_{ji}\dfrac{\partial W_{ij}}{\partial y_i} & y_{ji}\dfrac{\partial W_{ij}}{\partial y_i} \end{pmatrix} V_j \right)^{-1} \tag{6}$$

where $x_{ji} = x_j - x_i$, $y_{ji} = y_j - y_i$. For general cases with irregular particle distribution, variable smoothing length, and/or truncated boundary areas, the SPH particle approximation scheme with kernel gradient correction is of second order accuracy.

2.3 Water-soil interaction model

For modeling soil-water interaction, a coupling condition is necessary to treat the water and soil interface and to adapt their interactions. In this work, for every pair of interface water-soil particle, the following conditions need to be satisfied,

$$v_{water}^{\alpha} = v_{soil}^{\alpha} \tag{7}$$

$$p_{water} = p_{soil} \tag{8}$$

where the subscript "water" and "soil" denote field variables on water and soil particles respectively. To prevent possible unphysical penetration of particles from different materials, a penalty force similar to the Lennard-Jones repulsive force[14] from different materials near the interface is applied to particles when they are approaching. This force is applied pairwise to particles along their common axis as follows,

$$f\left(r_{ij}\right) = \begin{cases} D\left[\left(r_0/r_{ij}\right)^4 - \left(r_0/r_{ij}\right)^2\right]\left(x_{ij}/r_{ij}^2\right) & r_{ij} < r_0 \\ 0 & r_{ij} < r_0 \end{cases} \tag{9}$$

where D is a problem parameter which scales with the square of the largest velocity; r_0 is the cut-off distance, which is normally selected close to the initial spacing of particle; r_{ij} is the distance between the two particles; and x_{ij} is the vector position between the two particles.

3 EQUATIONS OF STATE AND CONSTITUTIVE MODELING

3.1 Equation of state of water

For water, the equation of state is applied with the following form Monaghan[14] when it was used for the free surface flows of water using SPH,

$$p = B\left[\left(\frac{\rho}{\rho_0}\right)^{\lambda} - 1\right] \tag{10}$$

where λ is a constant, and set equal to seven in most circumstances; ρ_0 is the reference density; B is a problem dependent parameter, which sets a limit for the maximum change of the density.

3.2 Constitutive modeling of soil

The modified Drucker-Prager[15][16] is used to model soil constitutive relation. Because elastic deformation of soil is small, in geotechnical problem, the plasticity stress-strain relations for soil are of great importance and frequently used for soil mechanics. In this study, non-associated flow rule and associated flow rule of the modified Drucker-Prager model are applied to model shear yielding and tensile yielding of the soil.

The total strain rate tensor of soil material $\dot{\varepsilon}$ is divided into two parts: an elastic strain rate tensor $\dot{\varepsilon}_e$ and a plastic strain rate tensor $\dot{\varepsilon}_p$,

$$\dot{\varepsilon}^{\alpha\beta} = \dot{\varepsilon}_e^{\alpha\beta} + \dot{\varepsilon}_p^{\alpha\beta} \tag{11}$$

Due to Hooke's law, the elastic strain rate tensor $\dot{\varepsilon}_e^{\alpha\beta}$ is followed,

$$\dot{\varepsilon}_e^{\alpha\beta} = \frac{\dot{s}^{\alpha\beta}}{2G} + \frac{1-2\upsilon}{E}\dot{\sigma}^m \delta^{\alpha\beta} \tag{12}$$

where $s^{\alpha\beta}$ is the deviatoric shear stress tensor; υ is Poisson's ratio; E is the elastic Young's modulus; G is the shear modulus and σ^m is the mean stress.

The plastic strain rate tensor is calculated by the plastic flow rule, which is given by for shear plastic flow:

$$\dot{\varepsilon}_p^{\alpha\beta} = \lambda^s \frac{\partial g^s}{\partial \sigma^{\alpha\beta}} \tag{13}$$

for tensile plastic flow:

$$\dot{\varepsilon}_p^{\alpha\beta} = \lambda^t \frac{\partial g^t}{\partial \sigma^{\alpha\beta}} \tag{14}$$

where λ^s is the rate form of shear plastic multiplier, λ^t is the rate form of tensile plastic multiplier, which can be specified from the consistency condition; and g^s is the shear plastic potential function, g^t is the tensile plastic potential function.

This study assumes that the yield surface is fixed in stress space, and plastic deformation occurs only if the stress state reaches the yield surface. Accordingly, the plastic deformation will occur while the following two yield criterions are satisfied,

$$f^s\left(I_1, J_2\right) = \sqrt{J_2} + q_\phi \sigma^m - k_c = 0 \tag{15}$$

$$f^t = \sigma^m - \sigma^t \tag{16}$$

where f^s and f^t are shear yield function and tensile yielding function; σ^t is tensile strength; I_1 and J_2 are, respectively, the first and second invariants of the stress tensor and deviatoric

shear stress tensor ; q_ϕ and k_c are Drucker-Prager constants, which are calculated from the Coulomb material constants c (cohesion) and ϕ (internal friction).
Substituting equations (12), (13), (14)into (11), and adopting the Jaumman stress rate for large deformation treatment, the stress-strain relationship for the current soil model at particle i can be derived to be,

$$\frac{d\sigma_i^{\alpha\beta}}{dt} = \sigma_i^{\alpha\gamma}\dot{\omega}_i^{\beta\gamma} + \sigma_i^{\gamma\beta}\dot{\omega}_i^{\alpha\gamma} + 2G_i\dot{e}_i^{\alpha\beta} + K_i\dot{\varepsilon}_i^{\gamma\gamma}\delta_i^{\alpha\beta} - \lambda_i^s\left[9K_i sin\psi_i\delta^{\alpha\beta} + \left(G/\sqrt{J_2}\right)_i s_i^{\alpha\beta}\right] \tag{17}$$

for shear plastic flow,

$$\frac{d\sigma_i^{\alpha\beta}}{dt} = \sigma_i^{\alpha\gamma}\dot{\omega}_i^{\beta\gamma} + \sigma_i^{\gamma\beta}\dot{\omega}_i^{\alpha\gamma} + 2G_i\dot{e}_i^{\alpha\beta} + K_i\dot{\varepsilon}_i^{\gamma\gamma}\delta_i^{\alpha\beta} - K_i\lambda_i^t\delta_i^{\alpha\beta} \tag{18}$$

for tensile plastic flow,
where $\dot{e}_i^{\alpha\beta} = \dot{\varepsilon}_i^{\alpha\beta} - \frac{1}{3}\dot{\varepsilon}_i^{\gamma\gamma}\delta_i^{\alpha\beta}$ is the deviatoric shear strain rate tensor; K is bulk modulus; ψ is the dilatancy angle. $\dot{\varepsilon}_i^{\alpha\beta}, \omega_i^{\alpha\beta}$ are the strain rate and spin rate tensors defined by

$$\dot{\varepsilon}_i^{\alpha\beta} = \frac{1}{2}\sum_j \frac{m_j}{\rho_j}\left[\left(v_j^\alpha - v_i^\alpha\right)\frac{\partial W_{ij}}{\partial x_i^\beta} + \left(v_j^\beta - v_i^\beta\right)\frac{\partial W_{ij}}{\partial x_i^\alpha}\right] \tag{19}$$

$$\Omega_i^{\alpha\beta} = \frac{1}{2}\sum_j \frac{m_j}{\rho_j}\left[\left(v_j^\alpha - v_i^\alpha\right)\frac{\partial W_{ij}}{\partial x_i^\beta} - \left(v_j^\beta - v_i^\beta\right)\frac{\partial W_{ij}}{\partial x_i^\alpha}\right] \tag{20}$$

The front soil constitutive model requires three soil parameters, the cohesion coefficient c, friction angle ϕ and elastic bulk modulus K, which can be specified from a simple experiment of shear box test or triaxial test.

4 NUMERICAL EXAMPLES

4.1 Water injection

In order to validate the SPH model, a numerical example of water injection is first given. The numerical results are compared with experimental observations by Kulasegaram et al. [7]. In the example, water is injected into a toric container from the bottom entrance at 18 m/s. Figure 1 shows the schematic illustration of the problem setup. Figure 2 shows the snapshots of the water injection process obtained using the presented SPH model and Figure 3 shows comparisons of the obtained SPH results (right column) with experimental observations (left column) and numerical results (middle column) from [7]. It is seen that the obtained SPH results agree well with results from experimental results.

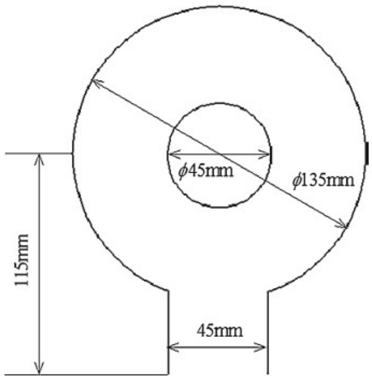

Figure 1: Schematic illustration of the water injection into a toric container.

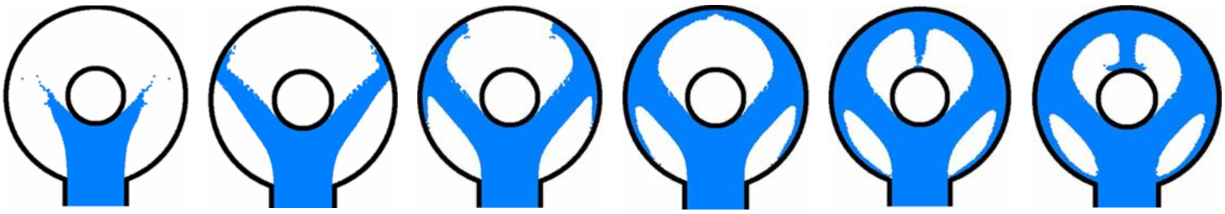

Figure 2: Snapshots of the water injection process.

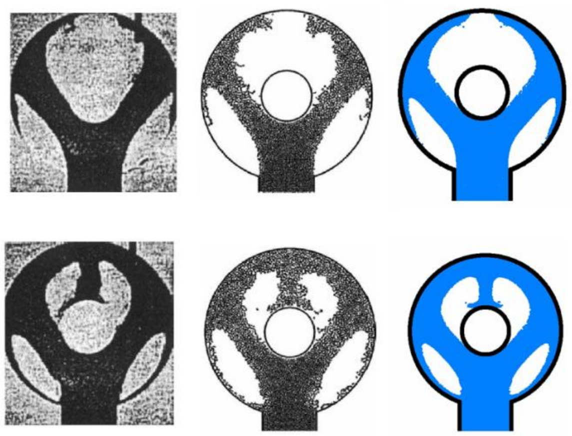

Figure 3: Comparisons of the obtained SPH results (right column) with experimental observations (left column) and numerical results (middle column) from [7].

4.2 Soil-water interaction

In this example, the SPH model is used for simulating soil-water interaction, in which a clump of soil is excavated by a water jet (see Figure 4). The rectangular shaped soil clump is of 2m long and 0.5m wide. The total number of soil particles is 14400 with the same initial smoothing length 0.0083m for each soil particle. The properties of the soil particles are as follows: density $\rho = 2500$ kg/m^3, Young's modulus E = 70 MPa and Poisson's ratio $\upsilon = 0.3$. There is an in-flow boundary for the water injection from the top of the soil clump (0.15 m away). Water particles are injected at 100 m/s, while the water particles are associated with density of $\rho = 1000$ kg/m^3 and a viscosity of $l = 10^{-3}$ Ns/m^2. The initial smoothing length of water particles is the same as that of the soil particles.

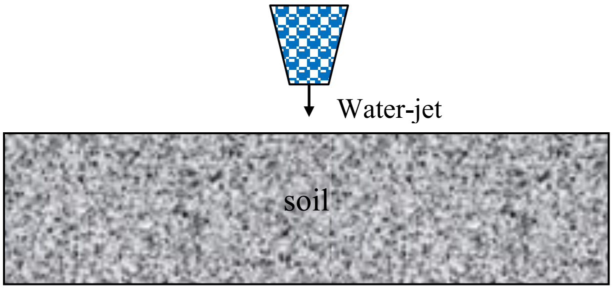

Figure 4: Schematically illustration of the soil excavation by water jet.

Figure 5 is the initial setup of the SPH model and Figure 6 shows the erosion process of soil excavation by water jet at representative times. In this simulation, the soil was easily eroded by the water jet and soil particles were splashed together with the water particles. Furthermore, the pit excavated by water jet became bigger and bigger with continuous flow in of water. The results of this simulation seem reasonable for both soil and water behavior. Because of the free boundary for soil, the soil particles near the boundary have large plastic deformation at the bottom of the rectangle during the calculation process.

Figure 5: Initial configuration of SPH model.

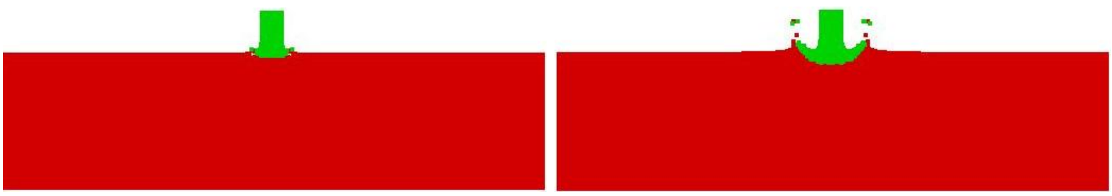

t=0.2s t=0.35s

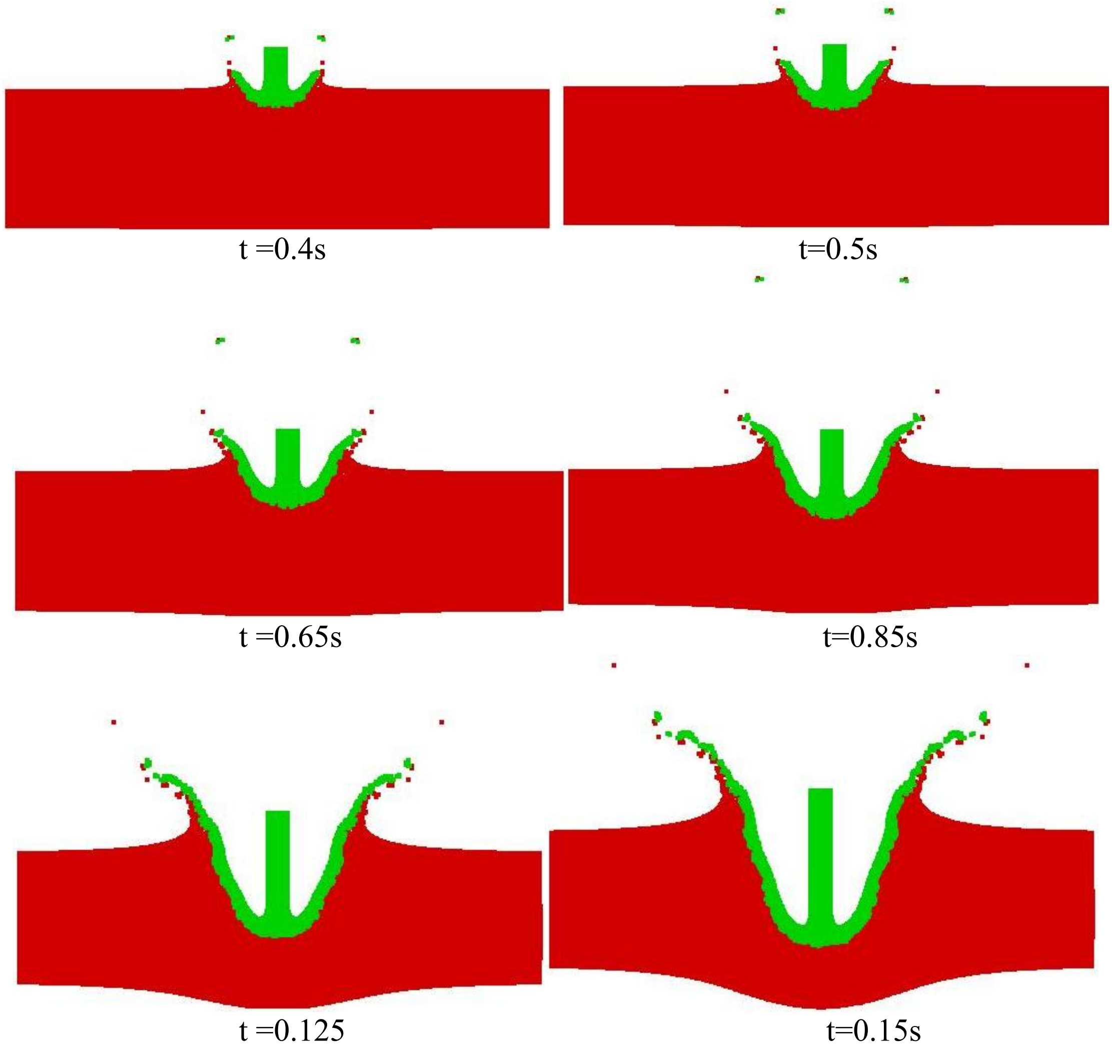

Figure 6: The erosion process of soil excavation by water jet.

5 CONCLUSIONS

In this paper, the SPH method is applied to model the soil-water interaction process. Fluid particles are used to model the free surface flows which are governed by Navier-Stokes equations, and soil particles are used to model the dynamic movement of soil, which is assumed to be an elastic–perfectly plastic material. The interaction of the neighboring fluid and soil particles renders the soil-water interaction without unphysical inter-particle penetrations. The preliminary results demonstrate that SPH method can well capture the inherent physics in soil-water interaction with large deformation and even break-up of soil and water surface in the soil excavation by water injection. More detailed investigations on quantitative analyses of soil-water interaction with different improved models will be conducted in the near future.

Acknowledgement *This work has been supported by the National Natural Science Foundation of China (11172306) and the 100 Talents Programme of the Chinese Academy of Sciences.*

REFERENCES

[1] L. B. Lucy, A numerical approach to the testing of the fission hypothesis, *Astron. J.*, **82** (12) (1977): 1013-1024.

[2] R. A. Gingold and J. J. Monaghan, Smoothed particle hydrodynamics-theory and application to non-spherical stars, *Mon. Not. R. Astron. Soc.*, **181** (1977): 375-389.

[3] J. J. Monaghan, Smoothed particle hydrodynamics, *Rep. Prog. Phys.*, **68** (8) (2005): 1703-1759.

[4] G. R. Liu and M. B. Liu. *Smoothed particle hydrodynamics: A meshfree particle method*. World Scientific, Singapore, (2003).

[5] M. B. Liu, G. R. Liu and K. Y. Lam, Constructing smoothing functions in smoothed particle hydrodynamics with applications, *J. Comput. Appl. Math.*, **155** (2) (2003): 263-284.

[6] J. R. Shao, H. Q. Li, G. R. Liu and M. B. Liu, An improved sph method for modeling liquid sloshing dynamics, *Comput. Struct.*, **100-101** (2012): 18-26.

[7] B. J. Kulasegaram S, Lewis RW, Profit M, Mould filling simulation in high pressure mould casting by meshless method. , *Fifth world congress on computational mechanics*, **Vienna, Austria** (2002).

[8] H.H. Bui, K.Sako, R. Fukagawa, Numerical simulation of soil-water interaction using smoothed particle hydrodynamics (SPH) method, Journal of Terramechanics 44 (2007) 339-346.

[9] T. Blanc, M. Pastor, A stabilized Fractional Step, Runge-Kutta Taylor SPH algorithm for coupled problems in geomechanics, Comput. Methods Appl. Mech. Engrg. 221-222 (2012) 41-53.

[10] M. Mabssout, M.I. Herreros, Runge – Kutta vs Taylor-SPH: Two time integration schemes for SPH with application to Soil Dynamics, Applied Mathematical Modelling 37 (2013) 3541-3563.

[11] J. J. Monaghan, Smoothed particle hydrodynamics, *Rep. Prog. Phys.*, **68** (8) (2005): 1703-1759.

[12] M. B. Liu, G. R. Liu and K. Y. Lam, Constructing smoothing functions in smoothed particle hydrodynamics with applications, *J. Comput. Appl. Math.*, **155** (2) (2003): 263-284.

[13] J. R. Shao, H. Q. Li, G. R. Liu and M. B. Liu, An improved sph method for modeling liquid sloshing dynamics, *Comput. Struct.*, **100-101** (2012): 18-26.

[14] J. J. Monaghan, Simulating free surface flows with SPH, *J. Comput. Phys.,* **110** (1994):399-406.

[15] H. H. Bui and K. Sako, SPH-Based Numerical Simulations for Large Deformation of Geomaterial Considering Soil-Structure Interaction, The 12th International Conference of International Association for Computer Methods and Advances in Geomechanics (IACMAG) 1-6 October, 2008 Goa, India.

[16] P. Huang, X. Zhang, S. Ma S and X. Huang, Contact Algorithms for the Material Point Method in Impact and Penetration Simulation, *Int. J. . Num. Meth. Eng.*, **85** (4) (2011): 498–517.